IN VIVO, COMPETITIVE BLOCKADE OF *N*-METHYL-D-ASPARTATE RECEPTORS INDUCES RAPID CHANGES IN FILAMENTOUS ACTIN AND DREBRIN A DISTRIBUTIONS WITHIN DENDRITIC SPINES OF ADULT RAT CORTEX

S. FUJISAWA,[a] T. SHIRAO[b] AND C. AOKI[a]*

[a]*Center for Neural Science, New York University, 4 Washington Place #809, New York, NY 10003, USA*

[b]*Department of Neurobiology and Behavior, Gunma University Graduate School of Medicine, 3-39-22 Showamachi, Maebashi 371, Japan*

Abstract—*In vitro* studies have demonstrated that prolonged *N*-methyl-D-aspartate receptor (NMDAR) blockade triggers a homeostatic up-regulation of NMDARs at synapses. Such upregulation can also be seen within 30 min *in vivo* in adult rats, implicating trafficking of reserve pools of NMDARs. Here, we evaluated the involvement of filamentous actin (F-actin), the major cytoskeletal component in spines, in this rapid *in vivo* homeostatic response, using biotinylated phalloidin as its probe. We also immuno-labeled spines for drebrin A, an F-actin-binding protein found at excitatory synapses and with a proposed role of modulating F-actin's cross-linking with one another and interactions with NMDARs. Quantitative 2-D analysis of ultrastructural images revealed that NMDAR blockade increased filamentous actin labeling per spine by 62.5% ($P<0.005$). The proportion of dendritic spines immuno-labeled for drebrin A also increased significantly, from 67.5% to 85% following NMDAR blockade ($P<0.001$), especially among larger spines. The frequency distributions of spine widths and postsynaptic density lengths were not affected by the D-(+)-2-amino-5-phosphonopentanoic acid (D-APV) treatment. However, the average postsynaptic density length was reduced by 25 nm among the fewer, drebrin A immuno-negative spines, indicating that drebrin A confers stability to synapse size. We propose that, in a homeostatic *in vivo* response, increases of drebrin A and F-actin within spines can enhance NMDAR trafficking by reducing cytoskeletal rigidity within the spine cytoplasm without changing the overt morphology of axo-spinous synapses. Alternatively or in addition, the cytoskeletal redistribution within spine cytoplasm may be triggered by the D-APV-induced, homeostatic up-regulation of NMDAR. © 2006 IBRO. Published by Elsevier Ltd. All rights reserved.

Key words: F-actin, drebrin, activity-dependent, trafficking, electron-microscopy, immunocytochemistry.

*Corresponding author. Tel: +1-212-998-3926; fax: +1-212-995-4011.
E-mail address: chiye@cns.nyu.edu (C. Aoki).
Abbreviations: AMPA, alpha-amino-3-hydroxy-5-methyl-4-isoxazole propionic acid; BSA, bovine-serum albumin; DAB, diaminobenzidine; D-APV, D-(+)-2-amino-5-phosphonopentanoic acid; EM, electron microscopy/electron microscope; F-actin, filamentous actin; L-APV, L-(+)-2-amino-5-phosphonopentanoic acid; LTP, long-term potentiation; NMDAR, *N*-methyl-D-aspartate receptor; PB, phosphate buffer; PBS, phosphate buffer saline; PSD, postsynaptic density; SIG, silver-intensified gold.

Dendritic spines exhibit high concentrations of cytoskeletal proteins, such as filamentous actin (F-actin) (Capani et al., 2001), and these proteins are believed to be involved in activity-dependent organization of synaptic molecules. For example, Fukazawa et al. (2003) showed that F-actin in spines is essential in long-term potentiation (LTP)-induced trafficking of alpha-amino-3-hydroxy-5-methyl-4-isoxazole propionic acid (AMPA) receptors. However, the involvement of cytoskeleton in activity-dependent trafficking of *N*-methyl-D-aspartate subtype of glutamate receptors (NMDARs) is not as well understood. Previous *in vitro* studies showing that NMDARs increase within dendritic spines in response to long-term NMDAR blockade (Rao and Craig, 1997; Turrigiano, 1999; Barria and Malinow, 2002; Carpenter-Hyland et al., 2004). Our laboratory has shown that a 30-minute *in vivo* application of an NMDAR antagonist, D-(+)-2-amino-5-phosphonopentanoic acid (D-APV), also produces a significant increase in the number of pre- and post-synaptic NR2A subunits and a concurrent decrease of synaptic NR2B subunits (Aoki et al., 2003; Fujisawa and Aoki, 2003). This rapid, homeostatic regulation of NMDAR may be achieved by trafficking of receptors along cytoskeletal tracts that connect the postsynaptic density (PSD) to the cytoplasm of spine heads and dendritic shafts. The current study examined D-APV-induced changes in the amount of two major cytoskeletal proteins within spines, namely, F-actin and the F-actin-binding protein, drebrin A.

F-actin functions as part of the PSD anchor for synaptic proteins, including NMDARs and drebrin. The disruption of F-actin drastically alters the localization of these molecules within spines (Adam and Matus, 1996; Allison et al., 1998, 2000), indicating that F-actin is also involved in intra-spine trafficking and endo/exocytosis of receptors (Kaech et al., 2001; Zhou et al., 2001; Qualmann et al., 2004). Reorganization of actin cytoskeleton is, in turn, initiated by changes in synaptic activity (van Rossum and Hanisch, 1999). Influx of extracellular Ca^{2+} via activation of NMDARs causes stabilization of F-actin (Star et al., 2002) and spine morphology (Ackermann and Matus, 2003; Brunig et al., 2004). Strong stimulation of NMDARs, however, induces massive depolymerization of F-actin and eventual collapse of dendritic spines (Rosenmund and Westbrook, 1993; Halpain et al., 1998). We surmised that F-actin within spines might be increased by the 30-min NMDAR blockade, and this promotes the intra-spinous trafficking of NMDARs.

We also hypothesized that receptor trafficking might be facilitated by the dissociation of NMDARs from the cytoskeletal anchors. α-Actinin-2 is known to anchor NMDARs onto actin cytoskeleton (Wyszynski et al., 1997; Dunah et al., 2000). An increase of another F-actin-binding protein, drebrin A, would competitively displace α-actinin-2 from F-actin, thus freeing receptors from cytoskeletal anchors and allowing them to relocate (review by Shirao and Sekino, 2001). Thus, we predicted that NMDAR blockade would increase intra-spinous levels of drebrin A and this event facilitates NMDAR trafficking within spines. Here, we report that our findings concur with these predictions about drebrin A and F-actin.

EXPERIMENTAL PROCEDURES

In vivo blockade of NMDARs in the cerebral cortex

We used tissues from brains of four animals prepared in our previous NMDAR-blockade experiments and prepared brains from four additional animals, using an alternative fixative (described below). *In vivo* application of NMDAR antagonist was as described previously (Aoki et al., 2003; Fujisawa and Aoki, 2003). Briefly, adult male Sprague–Dawley rats were anesthetized with 50 mg/kg of Nembutal. After stabilizing their heads in a stereotaxic apparatus, bilateral craniotomy and durotomy was performed over the medial parietal cortex. A small piece of Gelfoam (approximately 5 mm^2) soaked in 5 mM D-APV (Sigma, St. Louis, MO, USA) was placed above the durotomy site ($\sim$2 mm in length) in one hemisphere. The contralateral hemisphere received an equal-sized piece of Gelfoam soaked in an equal concentration of the inactive enantiomer, L-(+)-2-amino-5-phosphonopentanoic acid (L-APV) (Sigma). Both drugs were dissolved in artificial cerebrospinal fluid (115 mM NaCl, 3.3 mM KCl, 1 mM MgSO$_4$, 2 mM CaCl$_2$, 25.5 mM NaHCO$_3$, 1.2 mM NaH$_2$PO$_4$, 5 mM lactic acid, and 25 mM glucose). The drug application lasted for 30 min. All surgical procedures were in accordance with the National Institutes of Health Guide for the Care and Use of Experimental Animals and were approved by the NYU Animal Care and Use Committee. Care was taken to minimize the number of animals used and their suffering.

Tissue processing for ultrastructural analysis

At the end of drug application, the animals were perfused transcardially, first for 30 s with saline containing 300 USP units/ml of heparin (Henry Shine, NY, USA), followed immediately with the aldehydes. The perfusate was either 4% paraformaldehyde (EMS, Hatfield, PA, USA), mixed with 1% glutaraldehyde (EMS; therein called "glutaraldehyde-fixed") and dissolved in 0.1 M phosphate buffer (PB) (Aoki et al., 2003; Fujisawa and Aoki, 2003), or 4% paraformaldehyde alone (therein called "paraformaldehyde-fixed"). The brain was dissected out of the skull, and cut into 40 μm-thick sections using a vibratome. This procedure yielded approximately 20 vibratome sections that contained the cortical neuropil residing directly under the drug-soaked Gelfoam. All of these vibratome sections were stored, free-floating, in 0.01 M PB with 0.9% sodium chloride (phosphate buffer saline, PBS) and 0.05% sodium azide, at 4 °C.

Ultrastructural localization of F-actin and drebrin A for electron microscopy (EM)

F-actin was detected by its binding to biotinylated phalloidin (Molecular Probes, Eugene, OR, USA), while drebrin A was detected immunocytochemically using a well-characterized antibody (Aoki et al., 2005). First, the sections were freeze-thawed (see Aoki et al., 2003) in order to enhance penetration of histological reagents, then incubated in 1% hydrogen peroxide in PBS for 30 min and washed in PBS in order to minimize background labeling. Subsequently, the sections were incubated in 1% bovine-serum albumin in PBS (PBS–BSA) for 30 min in order to block non-specific binding of phalloidin or of the anti-drebrin A antibody.

We detected F-actin using silver-intensified gold (SIG) as the label. This label is non-diffusible and discrete, thus amenable to quantification and precise localization within single spines (Aoki et al., 2003). The sections were incubated in biotinylated phalloidin (Molecular Probes), diluted 1:20 in PBS–BSA with 0.05% sodium azide for 3 days at room temperature. After washes in PBS, tissues labeled with phalloidin were further incubated in a 1:100 dilution of 0.8 nm gold-conjugated goat anti-biotin antibody (EMS) for 3 h. Following post-fixation with 1% glutaraldehyde, the colloidal gold particles were intensified with silver (SIG), using the IntensEM Kit (Amersham, Arlington Heights, IL, USA). This procedure enlarges the gold particles to sizes detectable under the EM. Tissues labeled with phalloidin underwent osmium-free tissue processing to minimize loss of SIG labels (see Phend et al., 1995; Aoki et al., 2003).

The vibratome sections allotted for drebrin A immuno-labeling were processed for HRP–diaminobenzidine (DAB)-based labeling. HPR-DAB-based labels are diffusible and enzymatically amplified, thereby allowing for better detection of antigens. This label was chosen over SIG, because we wanted to optimize detection of the protein within spines, more than the precise localization or quantification within single spines. The tissues were incubated in PBS–BSA–azide solution containing a 1:1000 dilution of the anti-drebrin A antibody for 3 days at room temperature. After washes in PBS, these sections were incubated in a 1:200 dilution of secondary antibody, biotinylated goat anti-rabbit IgG (Vector, Burlingame, CA, USA) for 30 min, followed by PBS washes. Tissues were then incubated in the avidin–biotin complex solution (Elite Kit, Vector) for 30 min. Bound antibodies were visualized by the peroxidase reaction, using 0.3% 3,3′-DAB HCl in PBS with 0.01% hydrogen peroxide as a substrate. After washing in PBS, drebrin A-labeled tissues were fixed using 1% osmium tetroxide for 1 h.

Cytochemical control sections for both F-actin and drebrin labeling underwent the same procedures in parallel, except that they were incubated in PBS–BSA–azide without phalloidin or the drebrin A antibody.

The phalloidin- and drebrin A-labeled sections were dehydrated through incubations in ethanol and acetone, and then embedded in EMBed 812 (EMS). Drug-treated areas of the brain were determined by slight indentations of the cortex that resulted from craniotomy. Small areas of cortex ($\sim$1 mm in diameter) from the region immediately below the craniotomy were embedded in Beem capsules (2 vibratome sections from each animal). Previous studies showed that the D-APV-induced NMDAR redistribution was restricted to a 2 mm diameter of surface area immediately below the craniotomy (Aoki et al., 2003), and a depth extending down to layer 2 (Fujisawa and Aoki, 2003). The quantitative EM analysis in the current study was restricted to this zone showing the NMDAR trafficking. Each capsule was coded so that the experimental condition of each vibratome section would be unknown to the experimenter until the data analysis stage.

EM

Labeled tissues were cut into approximately 80 nm-thick sections using an ultramicrotome before examination under the EM (JEOL 1200XL, Japan). Conventional EM negatives or a digital camera (Hamamatsu CCD Camera, Japan; AMT, Danvers, MA, USA) were used to capture EM images from at least two grids per capsule. These images were taken in a systematically random

order for unbiased sampling, and in close proximity (within 5 μm) to the tissue–Epon interface, where labeling was most intense. At least two grids from each hemisphere from each animal were examined under the EM. For every animal, 40~80 pictures were taken for each experimental condition at 20,000~30,000× magnification. During the process of picture taking and the subsequent data collection, the experimenter had no knowledge of the treatment condition of the tissues being examined.

Data sampling: DAB and SIG labeling

We tallied the synapses in the electron micrographs in the order encountered. Asymmetric synapses were identified by the juxtaposition of two plasma membranes, with the presynaptic terminals containing synaptic vesicles, and the opposing profiles containing electron-dense PSDs.

Control tissues received no exposure to biotinylated phalloidin, but were incubated in a solution containing gold-conjugated anti-biotin antibodies. These displayed an extremely low level of non-specific, background labeling. Only one or two particles were observed within 20 μm^2 of the tissue captured by any single digital picture, and none of them fell on top of a synapse. Therefore, in F-actin-labeled tissues, a synapse was categorized as "labeled" if it contained even a single SIG particle within either the pre- or postsynaptic profile. In labeled synapses, the number of SIG particles within the pre- and postsynaptic profiles was recorded.

For drebrin-labeled tissues, synapses were categorized into one of three tiers, according to the intensity of the DAB reaction product. If the labeling filled the entire profile and was of strong intensity, the profile was categorized as "intensely labeled." If the labeling was discretely concentrated to a small area within the profile, or if it was of lighter intensity, the profile was categorized as "lightly labeled." Synapses with no detectable peroxidase reaction product were categorized as "not labeled."

Data sampling: spine widths and PSD lengths

In order to determine whether the 30-min D-APV blockade of NMDARs causes a change in the size of spines and synapses, we undertook a quantitative morphometric analysis. The ultra-thin sections used for these measurements were the same ones that had undergone immunolabeling for drebrin A. All of the tissue used for morphological analysis had undergone drebrin A-immunocytochemistry, followed by osmium tetroxide fixation. This set of tissue was chosen, because osmium post-fixation minimized tissue shrinkage. A minimum of two grids were used from each of the seven D-APV and the seven L-APV-treated hemispheres. As stated previously, these were derived from a systematically random selection of vibratome sections.

For measurements of spine widths and PSD lengths, we identified axo-spinous synapse profiles by the presence of PSDs, the spine apparatus and by the lack of mitochondria and microtubules in the postsynaptic profile. While we understand that there are large dendritic protrusions containing mitochondria and microtubules (Li et al., 2004), we excluded postsynaptic structures with these organelles, so that we could be sure to exclude dendritic shafts, many of which would be GABAergic and only sparsely spiny (White, 1989). Thus, by excluding the potentially GABAergic postsynaptic profiles from the sample, we were able to focus our analysis to excitatory synapses formed upon glutamatergic neurons (i.e. glutamate-to-glutamate connections). Synapses for which only a part of the spine was visible in the micrograph were also excluded from this analysis.

For each analyzable postsynaptic spine encountered within a single plane of section, we measured a drawn line that coursed parallel to the PSD at the widest point of the spine. The distance from one to the other end of the PSD darkening was measured using an Accutracker pen (Precision Technology Devices, IL,

USA), taking care to follow the PSD's curvature. The lengths of these lines in nanometers were calculated according to the magnification of the micrographs taken.

Unlike a 3-D morphometric analysis, such as the disector method, the 2-D analysis introduces two forms of bias: greater sampling of larger spines than of smaller ones, and inability to verify that spine widths are being measured at their widest points (Mouton, 2002). Indeed, a limited 3-D analysis of a dozen randomly encountered spines indicated that spine width measurements differed by about 20% compared with the outcome from 2-D analysis (data not shown). However, our aim was not to determine the absolute values of spine diameters or PSD lengths, but to determine whether the D-APV treatment caused a population shift in the size of synapses and spines, relative to the values observed within the L-APV-treated hemispheres. Moreover, we wished to use the same sample for analyzing whether the D-APV treatment had different effects upon drebrin A-immunoreactive versus drebrin A-negative spines. Since immunoreactivity is strongly influenced by the depth from the vibratome surface, we opted to sample widely and more efficiently using single-plane sections at portions that captured the resin-vibratome interfaces, rather than to perform 3-D reconstructions. Care was taken to use matched final magnifications to view and capture images from the D- and L-APV tissues.

Data analysis

In order to determine whether the proportion of F-actin- or drebrin-labeled synapses was different between the L-APV- and D-APV-treated tissues, we calculated the percentage of labeled synapses for every 20 synapses encountered. Student's t-test was used to determine the significance of differences between mean percentages of L- vs. D-APV tissues. Additionally, we also performed a Freeman-Tukey transformation method (Freeman and Tukey, 1950) of converting binomial data set into normal distributions. The results of this statistical test were similar to the t-test and thus are not shown.

When analyzing the differences in the number of F-actin-labeled SIG particles within single synapses, we grouped animals according to the aldehyde used for brain fixation. The two groups were 4% paraformaldehyde alone (will be referred to as the "paraformaldehyde-fixed tissue") and 4% paraformaldehyde plus 1% glutaraldehyde ("glutaraldehyde-fixed tissue"). The frequency distributions of average SIG particles per synapse were skewed heavily to the right regardless of the fixative used. Therefore, instead of using a parametric test to compare data from L- vs. D-APV tissues, we performed the non-parametric, Mann-Whitney U test. The group statistics were calculated by averaging the percent-changes from the L-APV data for each animal. The significance of the differences in percent-changes was tested using single-sample t-test, since the distributions were normal (data not shown).

The frequency distributions of spine widths and PSD lengths were normal, and therefore these sets of data from L-APV tissues and D-APV tissues were statistically compared using the Student's t-test.

Multiple linear regressions were performed to determine the degree of correlation between spine widths and PSD lengths.

RESULTS

NMDAR blockade induces an increase in the proportion of synapses labeled for F-actin using phalloidin

The cortical surfaces of adult rats were treated with a competitive NMDAR antagonist, D-APV, over one hemisphere and with its inactive enantiomer, L-APV, on the
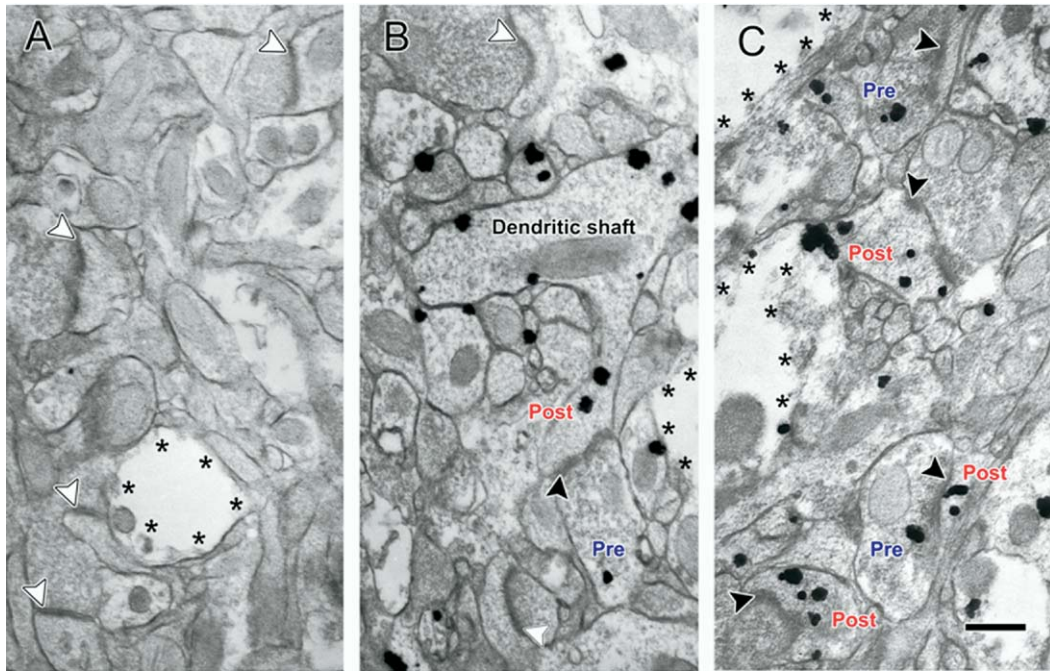
Fig. 1. Electron micrographs show phalloidin-labeling of F-actin in presynaptic axon terminals and postsynaptic spines of L-APV- and D-APV-treated tissues. The micrographs in these figures were derived from tissues of a paraformaldehyde-fixed animal, sampled strictly along the tissue-Epon interface (asterisks on the Epon-side). Arrowheads, indicating synapses, reside in the presynaptic terminals and point to PSDs. White arrowheads point to unlabeled synapses. Black arrowheads point to labeled synapses; i.e. those with one or more SIG particles in pre- and/or postsynaptic terminals. Post, postsynaptic spine; Pre, presynaptic axon terminal. Scale bar=200 nm. (A) Cytochemical control tissue from D-APV-treated hemisphere, incubated in a buffer lacking biotinylated phalloidin but containing gold-conjugated anti-biotin antibody. There was very little SIG labeling; none of them were found at synapses. (B) Pharmacological control, L-APV-treated tissue. Phalloidin labels were found in dendritic shafts, spines and axon terminals. Those found in dendritic spines were tallied as "postsynaptic labels," while those of the axon terminals were tallied as "presynaptic labels." In this example, two out of three synapses within this field show no detectable phalloidin-binding sites. (C) D-APV-treated tissue. More synapses were labeled with SIG particles and each labeled synapse contained more particles, compared with the L-APV-treated tissue.

contralateral hemisphere for 30 min. Aldehyde-fixed brain tissues from these animals were labeled for F-actin, using biotinylated phalloidin. Phalloidin was visualized with SIG particles, and their presence at drug-infused synapses in layer I of the cortex was determined by EM. Fig. 1B and C show examples of L- and D-APV-infused areas respectively, taken from one of four paraformaldehyde-fixed animals. Tissues from glutaraldehyde-fixed animals ($n=3$) exhibited relatively less labeling. In both types of tissues, SIG particles were observed in dendritic spines and axon terminals, as well as in dendritic shafts.

Since no synapse exhibited background SIG particles when phalloidin was omitted from the incubation cocktail (Fig. 1A), we were able to categorize a synapse as "labeled" (black arrowheads in Fig. 1), even if it contained only one SIG particle within its pre- or postsynaptic profile. When we calculated the average percentage of labeled synapses for every 20 synapses encountered in the L-APV-treated hemisphere, the paraformaldehyde-fixed tissues contained more synapses labeled with phalloidin ($40.3\pm1.8\%$ S.E.M.) than the glutaraldehyde-fixed tissues ($24.5\pm2.1\%$ S.E.M.; Fig. 2). Presumably, this difference in labeling reflects differences in accessibility of the phalloidin binding site brought about by the different fixation conditions. In both glutaraldehyde- ($t=4.78$, $df=63$, $P<0.001$) and paraformaldehyde-fixed tissues ($t=3.64$, $df=91$,

$P<0.001$), the proportion of F-actin-labeled synapses in the D-APV-treated area was increased significantly, compared with the L-APV-treated area, using Student's t-test (Fig. 2). This indicated that more synapses reached
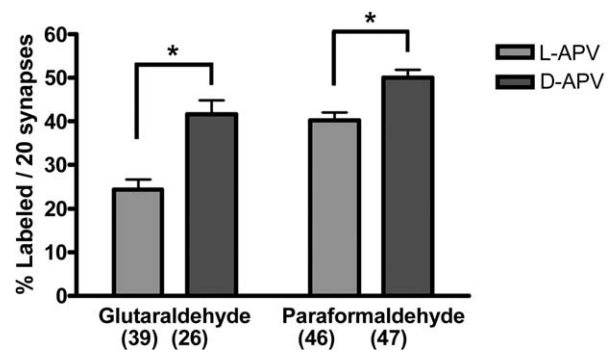

Fig. 2. The proportion of phalloidin-labeled synapses increases after D-APV application. For every 20 synapses encountered, the percentage of immuno-labeled synapses was calculated. The bar graphs show the mean percentage with S.E.M. as error bars. The numbers in parentheses below the bars correspond to the N for that data set. The distributions were compared between L-APV and D-APV treatments of single animals. Student's t-test showed significant increase in the proportion of labeled synapses, in both glutaraldehyde- and paraformaldehyde-fixed tissues. * Indicates $P<0.001$.
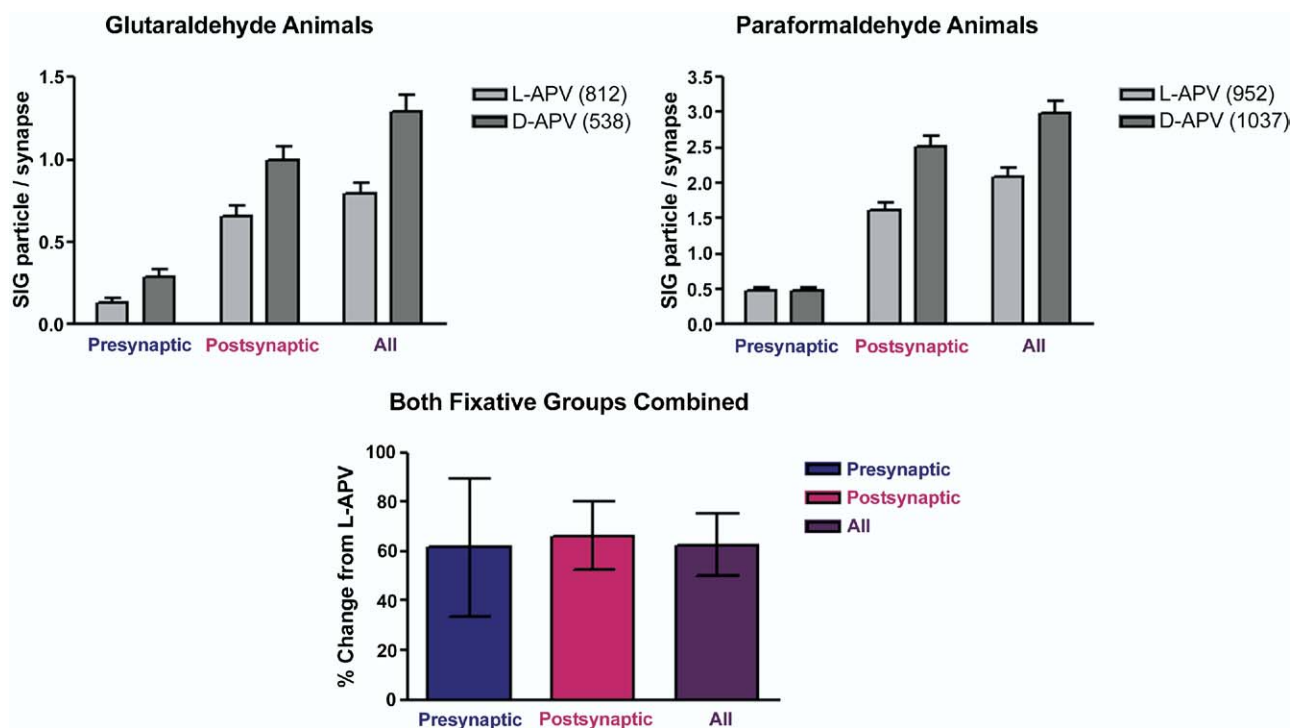
Fig. 3. The number of SIG particles labeling F-actin in the synaptic subcellular domains is greater in the D-APV-treated tissues. Top two graphs (A and B) represent the average number of SIG particles found within presynaptic profile, postsynaptic profile and across both micro-domains of each synapse ("All"). Data in graph A were taken from tissues of animals perfused with 4% paraformaldehyde–1% glutaraldehyde mixture ($n=3$). Data in graph B were from paraformaldehyde-fixed animals ($n=4$). Error bars show the standard error of means across synapses. Lighter-colored bars are data from L-APV-treated tissues from each animal, and darker-shaded bars are those from D-APV-treated tissues. The total number of synapses examined for both tissues is shown in parentheses next to the legend. Statistical analysis comparing L- and D-APV-treated tissues was performed for each micro-domain of each animal separately, using the non-parametric Mann-Whitney U test. Single asterisk indicates $P<0.001$. Panel C combines the data from both groups of data, by averaging the percent change from L-APV from all of the glutaraldehyde- and paraformaldehyde-fixed animals examined ($n=7$). Single-sample t-test was used to determine whether the changes were significantly different from zero; single star denotes $P<0.005$.

threshold level for F-actin detection, following the D-APV application.

NMDAR blockade induces an increase in the average number of F-actin labels within single synapses

We suspected that an increase in the number of synapses with detectable levels of F-actin reflects an increase in the amount of spinous F-actin within single synaptic profiles. Since SIG particles are quantifiable, we calculated the average number of SIG particles found within the following ultrastructural domains: within the presynaptic axon terminal, within the postsynaptic dendritic shaft or spine, and combined across both domains ("all"; Fig. 3). For each category, the average number of SIG particles per synapse was compared between the L- and D-APV-treated areas.

In glutaraldehyde-fixed brain tissues (Fig. 3A), SIG particles were less numerous in the presynaptic domain than in the postsynaptic domain. Comparisons across the drug treatments revealed a 63.3% greater density of SIG particles in the "all" category of the D-APV condition, relative to the L-APV condition ($z=5.15$, $df=1348$, $P<0.001$, Mann-Whitney U test). The D-APV condition exhibited an increase of SIG particles in the "presynaptic" ($z=2.16$,

$df=1348$, $P<0.05$) and "postsynaptic" ($z=3.98$, $df=1348$, $P<0.001$) micro-domains of synapses as well.

As seen in the glutaraldehyde-fixed tissue, the paraformaldehyde-fixed tissue (Fig. 3B) also exhibited less SIG particles in the presynaptic domain. Comparisons across the drug-treatment conditions revealed that SIG particles were significantly greater within postsynaptic profiles of the D-APV condition ($z=4.51$, $df=1987$, $P<0.001$), but not significantly different within presynaptic terminals ($z=0.49$, $df=1987$, $P>0.05$). In the combined "all" category, a significant increase by 43.1% followed the D-APV application ($z=4.25$, $df=1987$, $P<0.001$).

In order to analyze the overall trend across both fixative groups, the data from all animals ($n=7$) were combined by taking an average of percent-changes induced by the D-APV treatment, relative to the L-APV data, from each animal (Fig. 3C). Using single-sample t-test, we found a significant increase of SIG counts in the "postsynaptic" category (66.3%; $t=4.8$, $df=6$, $P<0.005$) and the "all" category (62.5%; $t=4.98$, $df=6$, $P<0.005$). Presynaptic counts also increased by the drug treatment, but the changes were too variable to be statistically significant ($t=2.19$, $df=6$, $P>0.05$). The data suggest that NMDAR blockade induces a greater, more consistent increase of
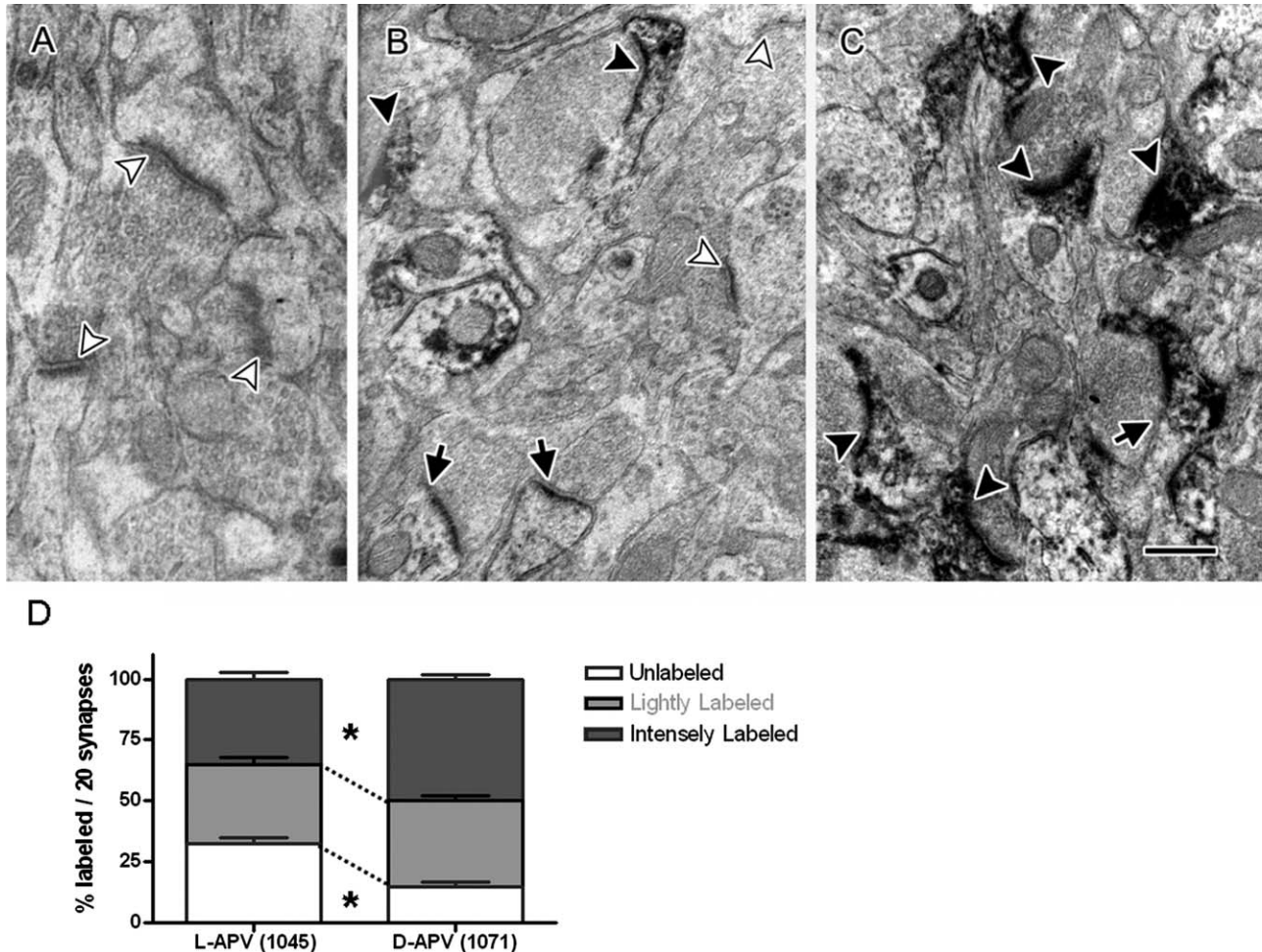
Fig. 4. D-APV treatment induces significant increases in drebrin A-labeled spines. All micrographs were taken from a representative animal. As with phalloidin-labeled tissues, pictures were taken along the tissue–Epon interface. All arrows indicating synapses are in presynaptic terminals, pointing at PSDs. White arrowheads point to unlabeled synapses; black arrows to lightly-labeled synapses; and black arrowheads to intensely-labeled synapses. Drebrin A labeling, when present, was always found within the postsynaptic profile and was never found presynaptically. (A) Control tissues incubated in a buffer without the primary antibody but otherwise treated identically to experimental tissue. No synapse was labeled by DAB (white arrows). (B) L-APV-treated tissue. Most synapses were labeled with DAB, but many of them were only lightly labeled (black arrows). (C) D-APV-treated tissue. There were more intensely labeled synapses (black arrowheads). (D) Each bar represents the proportion of unlabeled (white), lightly-labeled (gray) and intensely-labeled (dark gray) spines among all spines encountered (indicated in parentheses on the x axis). The proportion of unlabeled spines was significantly reduced within D-APV tissues, while the proportion of intensely-labeled synapses was significantly increased. Asterisk indicates $P<0.001$ by Student's t-test.

F-actin labels within postsynaptic profiles compared with presynaptic terminals.

NMDAR blockade increased the proportion of drebrin A-immunoreactive spines

We next evaluated whether the D-APV-induced increase of F-actin was accompanied by changes in drebrin A, an adult isoform of an F-actin-binding protein. In four glutaraldehyde-fixed animals, we immuno-labeled drebrin A with an isoform-specific antibody and visualized it with an immuno-peroxidase reaction product (Fig. 4B and C). There was not a single synapse whose presynaptic terminal was labeled for drebrin A but the majority of postsynaptic spines were immunolabeled. The average percentage of synapses lacking any immuno-labeling (white arrowheads in Fig. 4A and B) for every 20 synapses encountered was

32.5% in the L-APV-treated tissues and 15.0% in the D-APV-treated tissues. This decrease following D-APV treatment was statistically significant by the Student's t-test (Fig. 4D; $t=6.00$, $df=100$, $P<0.001$).

The peroxidase immuno-reaction product was categorized to be "intensely labeled" or "lightly labeled" depending on the extent and intensity of labeling within spines. Fig. 4 shows examples of intensely-labeled spines where the entire profile is filled with dark reaction product (Fig. 4B and C, black arrowheads). A lightly-labeled profile was so categorized when the reaction product was either only partially filled or was less intense (Fig. 4B and C, black arrows). Since the intensely- and lightly-labeled spines occurred within close proximity of one another, it is unlikely that this heterogeneity in the intensity of labeling resulted from varied degrees of penetration of immuno-reagents.
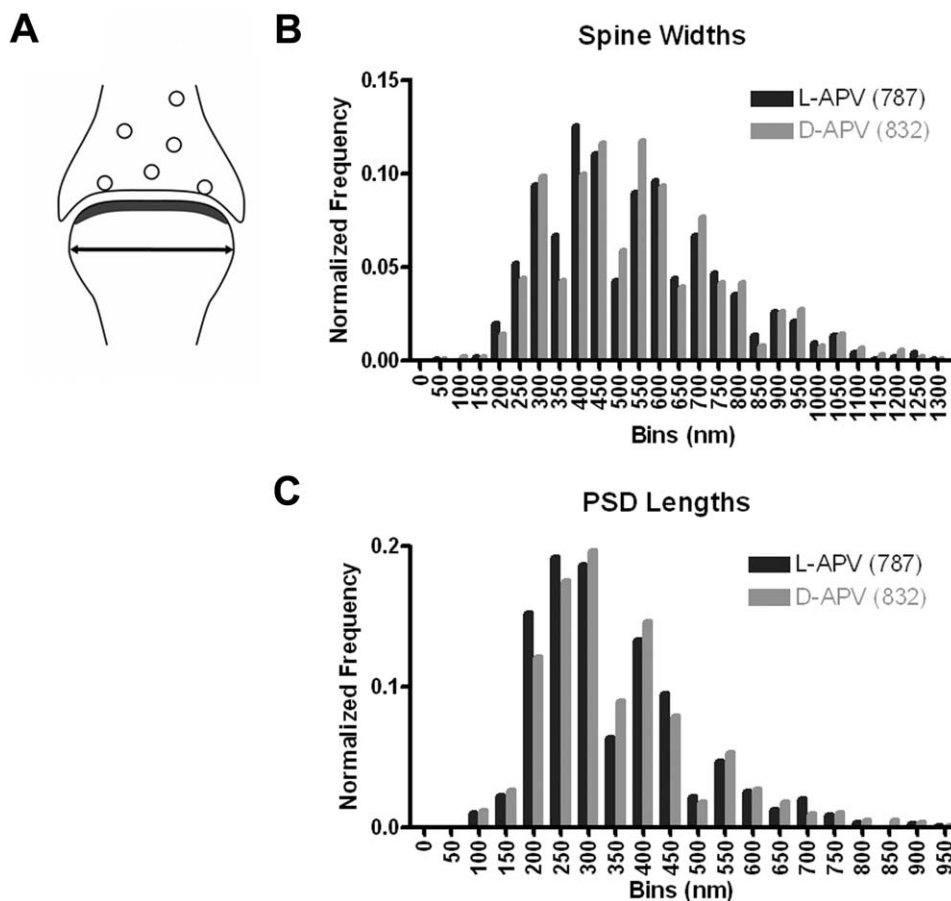
Fig. 5. D-APV treatment did not cause enlargement of spine heads or lengthening of PSDs. (A) Schematic drawing of how spine widths were measured on electron micrographs taken from glutaraldehyde- and osmium-fixed, drebrin immuno-labeled tissue. All spines encountered, whether or not drebrin A-labeled, were included in the sample. A line parallel to the PSD and postsynaptic membrane was drawn at the widest part of the spine head (arrow). Then length of this line was measured in nanometers. Additionally, the length of the PSD was measured by following any curvatures that were present along the synaptic cleft. (B, C) Normalized frequency distributions of spine widths and PSD lengths, respectively, binned by 50 nm. The numbers in parentheses in the legend represent the *N* for each group. There were no statistical differences in frequency distributions from the L- and D-APV tissues.

Rather, this heterogeneity is more likely to reflect varied amounts of drebrin A within spines, or differences in drebrin A's conformation that allow more antigenic sites to be available for antibody binding.

The proportion of intensely-labeled synapses was determined for every group of 20 randomly encountered synapses. Analysis of these groups revealed a significant increase in the proportion of intensely-labeled synapses following D-APV application ($t=4.79$, $df=100$, $P<0.001$; Fig. 4D). On the other hand, the proportion of lightly-labeled synapses did not change ($t=0.79$, $df=100$, $P>0.05$), suggesting that D-APV-induced increase in the number of drebrin A-immuno-positive synapses was due almost entirely to an increase of the intensely-labeled synapses.

NMDAR blockade does not induce morphological changes

Following an LTP-inducing protocol, an increase of F-actin within dendritic spines is accompanied by an increase in the volume of those spines (Matsuzaki et al., 2004). Although our pharmacological treatment was not an LTP-

inducing paradigm, we also observed an increase of F-actin within spines. Thus, we sought to determine whether D-APV induced changes in the apparent size of dendritic spine profiles and PSD profiles. 2-D analysis was chosen over 3-D analysis, so as to maximize the sample size within the zone that was both D-APV-treated and immunolabeled. (Further discussion of the rationale for this approach appears under "Experimental Procedures.")

Altogether we measured 1619 spine profiles. In L-APV-treated tissue, the average spine width (drebrin A-labeled and unlabeled, combined) was 538.5 nm (±7.6 nm S.E.M.) and ranged from 58.8 nm to 1323.5 nm. The mean spine width in the D-APV tissue was 551.8 nm (±7.4 nm S.E.M.) and ranged from 58.8 nm to 1323.5 nm (Fig. 5B). Student's *t*-test revealed that there is no significant difference in the spine-width distribution between the L-APV and the D-APV tissues ($t=1.24$, $df=1617$, $P>0.05$).

Analysis of PSD lengths from the same sample of spines showed that D-APV application did not induce any change in this parameter either ($t=0.87$, $df=1617$, $P>0.05$). The average PSD length in the L-APV tissue was

345.3 nm ($\pm$5.0 nm S.E.M.), ranging from 88.2 nm to 941.2 nm. In the D-APV tissue, PSD lengths had the same range of distribution, and the average length was 351.4 nm ($\pm$4.9 nm S.E.M.) (Fig. 5C).

Correlation between spine widths and PSD lengths was significant in the L-APV tissues ($r^2=0.589$, $P<0.001$), as tested by multiple regression analysis. As expected, the correlation between these two values remained significant in the D-APV tissues ($r^2=0.567$, $P<0.001$).

Spines containing drebrin A-immunoreactivity are larger and the larger spines are more likely to gain drebrin A-immunoreactivity following the NMDAR blockade

Although the average size of synapses remained the same, a possibility remained that a size change occurred within the subpopulation distinguishable by drebrin A-immunoreactivity.

We first noted that, in L-APV tissues, drebrin A immuno-positive spines were larger (567.4 ± 9.9 nm S.E.M.) and had longer PSDs (371.7 ± 6.2 nm S.E.M.) than those lacking drebrin A immunoreactivity (490.7 ± 11.4 nm S.E.M. for spine widths; 301.4 ± 7.1 nm S.E.M. for PSD lengths). These differences were significant, as tested by the Student's t-test ($t=4.93$, $df=785$, $P<0.001$ for spine widths; $t=6.99$, $df=785$, $P<0.001$ for PSD lengths). Similarly significant differences were found in spine widths and PSD lengths in the D-APV tissues ($t=5.13$, $df=830$, $P<0.001$ for spine widths; $t=7.04$, $df=830$, $P<0.001$ for PSD lengths).

NMDAR blockade induced a small reduction in the average spine width of drebrin A-negative synapses (25.2 nm reduction), compared with those in L-APV tissues, but this difference did not reach statistical significance ($t=-1.27$, $df=427$, $P>0.05$). The drug application also reduced the average PSD length of drebrin A-negative synapses by 27.4 nm, and this change reached statistical significance ($t=-2.23$, $df=427$, $P<0.05$). The PSD lengths of drebrin A-positive spines decreased following D-APV treatment, but to a smaller extent (by 5.6 nm). Widths of these drebrin A-immunoreactive spines were unaffected by the NMDAR blockade, increasing only by 0.8 nm. These results suggested that the drebrin A-positive spines are resistant to the D-APV-induced decrease of spine and PSD sizes.

Seeing that the D-APV treatment induced no significant overall changes in spine widths or PSD lengths, but did cause an increase in the proportion of spines with drebrin A-immunoreactivity, we then asked whether drebrin A-immunoreactivity increased similarly across spines of different sizes. To address this question, we categorized spines into two: those with diameter greater than 700 nm and those with diameter less than 700 nm. A comparison across the two size groups revealed that larger spines were more likely to contain drebrin A, as seen within the L-APV tissue ($t=4.23$, $df=38$, $P<0.001$). D-APV-induced increase of drebrin A-immunoreactivity was greater among the larger spines (by 61.1%) than the smaller spines (by 54.5%). Altogether, these observations indicated that larger spines are more likely to be drebrin A-immunoreac-

tive and are also more likely to gain drebrin A-immunoreactivity following NMDAR blockade.

DISCUSSION

Previously, our laboratory showed that 30-minutes of *in vivo* NMDAR blockade causes trafficking of the NR2A subunits of NMDARs into the synaptic area and of the NR2Bs away from synapses (Aoki et al., 2003; Fujisawa and Aoki, 2003). In the present study, we have demonstrated that the same manipulation also causes changes in the distribution of cytoskeletal proteins, especially within the larger spines, without causing overt changes in the size of spines or PSDs.

NMDAR blockade alters cytoskeletal distribution: postsynaptic impact

We have shown that both the number of synapses labeled with phalloidin and the density of labeling within single synaptic profiles significantly increased following NMDAR blockade (Figs. 2 and 3). How might the increased F-actin level contribute to the homeostatic up-regulation of NMDARs? Compared with AMPA receptors, relatively little is known about the trafficking of NMDAR within spines (Wu et al., 2002; Schulz et al., 2004; Wierenga et al., 2005). F-actin allows vesicles to traffic via myosin motor proteins (Baker and Titus, 1998; Wu et al., 2002) and these myosin motor proteins have been localized to spines (Morales and Fifkova, 1989; Walikonis et al., 2000). Although NMDARs have not been identified as cargoes, Naisbitt et al. (2000) have shown that PSD-95, a scaffolding protein often associated with NMDARs, is trafficked along F-actin via myosin-V. For trafficking up to the spine but not within spines, Hirokawa's group has identified KIF-17-containing motor protein complexes that carry NR2B subunits along microtubules in the dendrites (Setou et al., 2000; Guillaud et al., 2003). Taken together, the increased F-actin observed within D-APV-blocked spines may facilitate the movement of NMDAR-containing vesicles within spines relatively more than in dendritic shafts.

NMDAR blockade alters cytoskeletal distribution: presynaptic impact

We have demonstrated here that D-APV induces an increase of F-actin within terminals, albeit to a lesser degree than within spines. Perhaps the lack of postsynaptic NMDAR activity is reported back to the presynaptic terminal via retrograde signaling, and the presynaptic terminal increases F-actin in order to maintain homeostasis. How might axonal F-actin be involved in the maintenance of homeostasis?

F-actin's role within axon terminals remains unclear (Doussau and Augustine, 2000; Halpain, 2003). Some studies suggest that neurotransmitter vesicles are trafficked along actin filaments via myosin (Evans et al., 1998). F-actin may also be involved in vesicle recycling (Shupliakov et al., 2002), scaffolding of vesicles (Sankaranarayanan et al., 2003) and/or vesicular release (Cole et al., 2000). Increased levels of F-actin in the terminals may enhance these vesicular func-

tions and, together, increase neurotransmitter release as a response to NMDAR blockade.

Increased F-actin in terminals may also facilitate the trafficking of presynaptic NMDARs. NMDARs are present in the axon terminals as autoreceptors (Woodhall et al., 2001; Sjostrom et al., 2003), and we have seen changes in the distribution of these receptors within axons following D-APV applications (Aoki et al., 2003; Fujisawa and Aoki, 2003).

NMDAR blockade may create a plastic cytoskeletal environment via drebrin A

Drebrin A is the adult form of an F-actin-binding protein that is found exclusively in postsynaptic compartments of excitatory synapses (Fig. 4B and C, also see Aoki et al., 2005). In this study, we have shown that 30 min of NMDAR blockade causes a significant increase in the proportion of synapses immuno-labeled for drebrin A (Fig. 4D). This increase is likely to reflect the influx of drebrin A from dendritic shafts. De novo synthesis of drebrin A is less likely, since the D-APV treatment was brief. It is possible that conformational changes have also taken place, yielding enhanced immunoreactivity of the protein.

What does the observed increase of drebrin A immunolabeling signify? Firstly, drebrin A competes with α-actinin-2 for actin-binding. α-Actinin-2 is another dynamic PSD protein (Nakagawa et al., 2004) with binding sites for both F-actin and NMDARs (Wyszynski et al., 1997; Dunah et al., 2000). If α-actinin-2 anchors synaptic NMDARs onto the actin cytoskeleton, and if the observed increase of drebrin A (due to increased protein level or possibly also due to conformational changes) leads to greater displacement α-actinin-2 from the actin cytoskeleton, this disruption may free NMDARs to be trafficked into or out of the synaptic zone (review by Shirao and Sekino, 2001).

Besides linking NMDARs to the cytoskeleton, α-actinin-2 also has an actin cross-linking activity (Dunah et al., 2000; Gimona et al., 2002). With drebrin preventing α-actinin-2 from bundling the actin filaments (Ishikawa et al., 1994), the actin cytoskeleton may be more mobile and plastic, thereby allowing for increased trafficking of NMDARs within spines.

Drebrin also competes with tropomyosin for actin-binding (Ishikawa et al., 1994). Tropomyosin, when bound to actin, protects actin filaments from actin-destabilizing agents. Since increased drebrin A levels should reduce the number of tropomyosin-actin complex, we suggest that actin cytoskeleton in D-APV-treated spines could be more susceptible to severing. Perhaps this is a necessary condition to allow filaments to break free of a rigid organization and then enhance motility of NMDARs within spines.

An increase of drebrin is associated with various types of plasticity. For example, increased levels of drebrin are observed in the stimulated layers of the hippocampus after *in vivo* LTP induction (Fukazawa et al., 2003). Conversely, cultured hippocampal neurons with decreased levels of drebrin A expression fail to exhibit the D-APV-induced elevation of NMDARs within spines (Takahashi et al., 2005). Drebrin A is also known to be highly expressed in spines that are just maturing (Takahashi et al., 2003; Aoki et al.,

2005). In contrast, drebrin is found in low amounts in brains of Alzheimer's or Down syndrome patients (Harigaya et al., 1996; Hatanpaa et al., 1999; Shim and Lubec, 2002). Our present finding leads us to believe that there is a yet unknown cascade within spines that forms a tight link between cytoskeletal changes via drebrin A and synaptic strength modifications.

NMDAR blockade does not trigger enlargement of spines, but larger spines exhibit greater cytoplasmic plasticity

Since increases in F-actin labeling and over-expression of drebrin A are both known to promote morphological plasticity in spines (Hayashi and Shirao, 1999; Takahashi et al., 2003; Matsuzaki et al., 2004; Mizui et al., 2005), we predicted that the size of spines may change following D-APV application. However, this was not the case. When spine widths and PSD lengths were measured from micrographs, we observed that, despite the apparent increases in cytoskeletal proteins, D-APV application did not induce morphological changes in spines. If anything, the D-APV treatment caused a slight decrease of PSD lengths. This size reduction was measurable only among the population of spines lacking drebrin A. Since the D-APV treatment increased the population of drebrin A-immunoreactive spines, drebrin A may have conferred morphological stability upon an increasing sub-population of spines. These PSD-length reductions among the drebrin A-negative spines did not result in a significant shift in the overall size of spines and PSDs, presumably because the drebrin A-negative spines are much fewer in number. A separate study from our laboratory supports the idea that drebrin A may have a stabilizing influence upon spines (Mahadomrongkul et al., 2005). Together, these findings indicate that drebrin A may stabilize overt morphology, such as the size of spines and PSDs, while also redirecting the intracellular organization of F-actin toward a state favoring trafficking of synaptic proteins, such as the NR2A and NR2B subunits of NMDARs.

There are a number of explanations for why overt morphological changes did not accompany increases in cytoskeletal proteins in this study. One possibility is the one we alluded to earlier, namely that the increases in the cytological detection of the proteins may have been caused by conformational changes, with or without changes in the overall levels of F-actin or of drebrin A. One approach that is tailored more toward measuring protein levels is Western blot analyses. However, studies comparing Western blot data with EM immunocytochemical analyses of spine proteins indicate that neither is a good predictor of the other (Harigaya et al., 1996; Rodrigues et al., 2004; Mahadomrongkul et al., 2005). Such differences in outcomes might be expected, since Western blot analyses cannot exclude proteins residing at subcellular domains outside of spines, while EM-ICC cannot distinguish altered levels of protein detection derived from conformational changes versus protein level changes.

Another explanation for the lack of apparent changes in spine widths is that 2-D analyses fail to detect changes

in spine shapes. However, this explanation seems unlikely, because we could already detect small changes (25 nm, 7.5% change) in PSD lengths within a sample size of 429, or roughly one-quarter of the sample size of all spines encountered. This sample size was likely to have been large enough to minimize the variance of the data (Umbriaco et al., 1994) and detect changes, if there were any.

It is possible that the amount of increases in cytoskeletal proteins triggered by NMDAR blockade is much less than those evoked by LTP-inducing protocols. What we have shown is that changes in the intracellular environment of spines may be separable from the overt changes in spine shape or size.

Molecular steps leading to cytoskeletal reorganization must be explored

Other studies have also shown that prolonged changes in NMDAR activity lead to cytoskeletal reorganization. Matus's group has shown that influx of Ca^{2+} via NMDAR stimulation leads to reduced spine motility (Brunig et al., 2004), and conversely, others have pointed to a link between reduced NMDAR activity and increased spine motility (Fischer et al., 2000; Burrone et al., 2002; Star et al., 2002; Ackermann and Matus, 2003). Together, we hypothesize that decreased levels of NMDAR-mediated synaptic activity may be the trigger that initiates cytoskeletal changes. In the case of the current study, this reorganization may facilitate or be required for trafficking of NMDARs.

Since AMPA-to-NMDA receptor ratio is maintained well following LTP in cortical synapses (Watt et al., 2000), the mechanism regulating NMDAR trafficking may overlap with that for trafficking of AMPA receptors that occur during the late phase of LTP. Matsuzaki's (2004) group and others (Toni et al., 2001; Okamoto et al., 2004) have repeatedly shown that LTP induction increases spine size and F-actin content. This cytoskeletal plasticity seems to be crucial in trafficking of AMPA receptors for the maintenance LTP (Fukazawa et al., 2003). Perhaps accelerated polymerization of actin is required whenever there is an increased targeting of receptors into spine heads, regardless of how receptor trafficking is triggered (by LTP or by smaller changes associated with homeostasis). However, molecular mechanisms that initiate cytoskeletal reorganization are not well understood and await further research.

REFERENCES

Ackermann M, Matus A (2003) Activity-induced targeting of profilin and stabilization of dendritic spine morphology. Nat Neurosci 6:1194–1200.

Adam G, Matus A (1996) Role of actin in the organisation of brain postsynaptic densities. Brain Res Mol Brain Res 43:246–250.

Allison DW, Chervin AS, Gelfand VI, Craig AM (2000) Postsynaptic scaffolds of excitatory and inhibitory synapses in hippocampal neurons: maintenance of core components independent of actin filaments and microtubules. J Neurosci 20:4545–4554.

Allison DW, Gelfand VI, Spector I, Craig AM (1998) Role of actin in anchoring postsynaptic receptors in cultured hippocampal neurons: differential attachment of NMDA versus AMPA receptors. J Neurosci 18:2423–2436.

Aoki C, Fujisawa S, Mahadomrongkul V, Shah PJ, Nader K, Erisir A (2003) NMDA receptor blockade in intact adult cortex increases trafficking of NR2A subunits into spines, postsynaptic densities, and axon terminals. Brain Res 963:139–149.

Aoki C, Sekino Y, Hanamura K, Fujisawa S, Mahadomrongkul V, Ren Y, Shirao T (2005) Drebrin A is a postsynaptic protein that localizes in vivo to the submembranous surface of dendritic sites forming excitatory synapses. J Comp Neurol 483:383–402.

Baker JP, Titus MA (1998) Myosins: matching functions with motors. Curr Opin Cell Biol 10:80–86.

Barria A, Malinow R (2002) Subunit-specific NMDA receptor trafficking to synapses. Neuron 35:345–353.

Brunig I, Kaech S, Brinkhaus H, Oertner TG, Matus A (2004) Influx of extracellular calcium regulates actin-dependent morphological plasticity in dendritic spines. Neuropharmacology 47:669–676.

Burrone J, O'Byrne M, Murthy VN (2002) Multiple forms of synaptic plasticity triggered by selective suppression of activity in individual neurons. Nature 420:414–418.

Capani F, Martone ME, Deerinck TJ, Ellisman MH (2001) Selective localization of high concentrations of F-actin in subpopulations of dendritic spines in rat central nervous system: a three-dimensional electron microscopic study. J Comp Neurol 435:156–170.

Carpenter-Hyland EP, Woodward JJ, Chandler LJ (2004) Chronic ethanol induces synaptic but not extrasynaptic targeting of NMDA receptors. J Neurosci 24:7859–7868.

Cole JC, Villa BR, Wilkinson RS (2000) Disruption of actin impedes transmitter release in snake motor terminals. J Physiol 525 (Pt 3): 579–586.

Doussau F, Augustine GJ (2000) The actin cytoskeleton and neurotransmitter release: an overview. Biochimie 82:353–363.

Dunah AW, Wyszynski M, Martin DM, Sheng M, Standaert DG (2000) Alpha-actinin-2 in rat striatum: localization and interaction with NMDA glutamate receptor subunits. Brain Res Mol Brain Res 79:77–87.

Evans LL, Lee AJ, Bridgman PC, Mooseker MS (1998) Vesicle-associated brain myosin-V can be activated to catalyze actin-based transport. J Cell Sci 111 (Pt 14):2055–2066.

Fischer M, Kaech S, Wagner U, Brinkhaus H, Matus A (2000) Glutamate receptors regulate actin-based plasticity in dendritic spines. Nat Neurosci 3:887–894.

Freeman MF, Tukey JW (1950) Transformations related to the angular and the square root. Ann Math Stat 21:607–611.

Fujisawa S, Aoki C (2003) In vivo blockade of N-methyl-D-aspartate receptors induces rapid trafficking of NR2B subunits away from synapses and out of spines and terminals in adult cortex. Neuroscience 121:51–63.

Fukazawa Y, Saitoh Y, Ozawa F, Ohta Y, Mizuno K, Inokuchi K (2003) Hippocampal LTP is accompanied by enhanced F-actin content within the dendritic spine that is essential for late LTP maintenance in vivo. Neuron 38:447–460.

Gimona M, Djinovic-Carugo K, Kranewitter WJ, Winder SJ (2002) Functional plasticity of CH domains. FEBS Lett 513:98–106.

Guillaud L, Setou M, Hirokawa N (2003) KIF17 dynamics and regulation of NR2B trafficking in hippocampal neurons. J Neurosci 23: 131–140.

Halpain S (2003) Actin in a supporting role. Nat Neurosci 6:101–102.

Halpain S, Hipolito A, Saffer L (1998) Regulation of F-actin stability in dendritic spines by glutamate receptors and calcineurin. J Neurosci 18:9835–9844.

Harigaya Y, Shoji M, Shirao T, Hirai S (1996) Disappearance of actin-binding protein, drebrin, from hippocampal synapses in Alzheimer's disease. J Neurosci Res 43:87–92.

Hatanpaa K, Isaacs KR, Shirao T, Brady DR, Rapoport SI (1999) Loss of proteins regulating synaptic plasticity in normal aging of the human brain and in Alzheimer disease. J Neuropathol Exp Neurol 58:637–643.

Hayashi K, Shirao T (1999) Change in the shape of dendritic spines caused by overexpression of drebrin in cultured cortical neurons. J Neurosci 19:3918–3925.

Ishikawa R, Hayashi K, Shirao T, Xue Y, Takagi T, Sasaki Y, Kohama K (1994) Drebrin, a development-associated brain protein from rat embryo, causes the dissociation of tropomyosin from actin filaments. J Biol Chem 269:29928–29933.

Kaech S, Parmar H, Roelandse M, Bornmann C, Matus A (2001) Cytoskeletal microdifferentiation: a mechanism for organizing morphological plasticity in dendrites. Proc Natl Acad Sci U S A 98:7086–7092.

Li Z, Okamoto K, Hayashi Y, Sheng M (2004) The importance of dendritic mitochondria in the morphogenesis and plasticity of spines and synapses. Cell 119:873–887.

Mahadomrongkul V, Huerta PT, Shirao T, Aoki C (2005) Stability of the distribution of spines containing drebrin A in the sensory cortex layer I of mice expressing mutated APP and PS1 genes. Brain Res 1064:66–74.

Matsuzaki M, Honkura N, Ellis-Davies GC, Kasai H (2004) Structural basis of long-term potentiation in single dendritic spines. Nature 429:761–766.

Mizui T, Takahashi H, Sekino Y, Shirao T (2005) Overexpression of drebrin A in immature neurons induces the accumulation of F-actin and PSD-95 into dendritic filopodia, and the formation of large abnormal protrusions. Mol Cell Neurosci 30:149–157.

Morales M, Fifkova E (1989) In situ localization of myosin and actin in dendritic spines with the immunogold technique. J Comp Neurol 279:666–674.

Mouton P (2002) Principles and practices of unbiased stereology. Baltimore: Johns Hopkins University Press.

Naisbitt S, Valtschanoff J, Allison DW, Sala C, Kim E, Craig AM, Weinberg RJ, Sheng M (2000) Interaction of the postsynaptic density-95/guanylate kinase domain-associated protein complex with a light chain of myosin-V and dynein. J Neurosci 20:4524–4534.

Nakagawa T, Engler JA, Sheng M (2004) The dynamic turnover and functional roles of alpha-actinin in dendritic spines. Neuropharmacology 47:734–745.

Okamoto K, Nagai T, Miyawaki A, Hayashi Y (2004) Rapid and persistent modulation of actin dynamics regulates postsynaptic reorganization underlying bidirectional plasticity. Nat Neurosci 7:1104–1112.

Phend KD, Rustioni A, Weinberg RJ (1995) An osmium-free method of epon embedment that preserves both ultrastructure and antigenicity for post-embedding immunocytochemistry. J Histochem Cytochem 43:283–292.

Qualmann B, Boeckers TM, Jeromin M, Gundelfinger ED, Kessels MM (2004) Linkage of the actin cytoskeleton to the postsynaptic density via direct interactions of Abp1 with the ProSAP/Shank family. J Neurosci 24:2481–2495.

Rao A, Craig AM (1997) Activity regulates the synaptic localization of the NMDA receptor in hippocampal neurons. Neuron 19:801–812.

Rodrigues SM, Farb CR, Bauer EP, LeDoux JE, Schafe GE (2004) Pavlovian fear conditioning regulates Thr286 autophosphorylation of Ca2+/calmodulin-dependent protein kinase II at lateral amygdala synapses. J Neurosci 24:3281–3288.

Rosenmund C, Westbrook GL (1993) Calcium-induced actin depolymerization reduces NMDA channel activity. Neuron 10:805–814.

Sankaranarayanan S, Atluri PP, Ryan TA (2003) Actin has a molecular scaffolding, not propulsive, role in presynaptic function. Nat Neurosci 6:127–135.

Schulz TW, Nakagawa T, Licznerski P, Pawlak V, Kolleker A, Rozov A, Kim J, Dittgen T, Kohr G, Sheng M, Seeburg PH, Osten P (2004) Actin/{alpha}-actinin-dependent transport of AMPA receptors in dendritic spines: role of the PDZ-LIM protein RIL. J Neurosci 24:8584–8594.

Setou M, Nakagawa T, Seog D-H, Hirokawa N (2000) Kinesin superfamily motor protein KIF17 and mLin-10 in NMDA receptor-containing vesicle transport. Science 288:1796–1802.

Shim KS, Lubec G (2002) Drebrin, a dendritic spine protein, is manifold decreased in brains of patients with Alzheimer's disease and Down syndrome. Neurosci Lett 324:209–212.

Shirao T, Sekino Y (2001) Clustering and anchoring mechanisms of molecular constituents of postsynaptic scaffolds in dendritic spines. Neurosci Res 40:1–7.

Shupliakov O, Bloom O, Gustafsson JS, Kjaerulff O, Low P, Tomilin N, Pieribone VA, Greengard P, Brodin L (2002) Impaired recycling of synaptic vesicles after acute perturbation of the presynaptic actin cytoskeleton. Proc Natl Acad Sci U S A 99:14476–14481.

Sjostrom PJ, Turrigiano GG, Nelson SB (2003) Neocortical LTD via coincident activation of presynaptic NMDA and cannabinoid receptors. Neuron 39:641–654.

Star EN, Kwiatkowski DJ, Murthy VN (2002) Rapid turnover of actin in dendritic spines and its regulation by activity. Nat Neurosci 5:239–246.

Takahashi H, Mizui T, Shirao T (2005) Down-regulation of drebrin A expression suppresses synaptic targeting of NMDA receptors in developing hippocampal neurones. J Neurochem. 97(S1):110–115. doi:10.1111/j.1471-4159.2005.03536x.

Takahashi H, Sekino Y, Tanaka S, Mizui T, Kishi S, Shirao T (2003) Drebrin-dependent actin clustering in dendritic filopodia governs synaptic targeting of postsynaptic density-95 and dendritic spine morphogenesis. J Neurosci 23:6586–6595.

Toni N, Buchs P-A, Nikonenko I, Povilaitite P, Parisi L, Muller D (2001) Remodeling of synaptic membranes after induction of long-term potentiation. J Neurosci 21:6245–6251.

Turrigiano GG (1999) Homeostatic plasticity in neuronal networks: the more things change, the more they stay the same. Trends Neurosci 22:221–227.

Umbriaco D, Watkins KC, Descarries L, Cozzari C, Hartman BK (1994) Ultrastructural and morphometric features of the acetylcholine innervation in adult rat parietal cortex: an electron microscopic study in serial sections. J Comp Neurol 348:351–373.

van Rossum D, Hanisch UK (1999) Cytoskeletal dynamics in dendritic spines: direct modulation by glutamate receptors? Trends Neurosci 22:290–295.

Walikonis RS, Jensen ON, Mann M, Provance DW Jr, Mercer JA, Kennedy MB (2000) Identification of proteins in the postsynaptic density fraction by mass spectrometry. J Neurosci 20:4069–4080.

Watt AJ, van Rossum MC, MacLeod KM, Nelson SB, Turrigiano GG (2000) Activity coregulates quantal AMPA and NMDA currents at neocortical synapses. Neuron 26:659–670.

White E (1989) Cortical circuits: synaptic organization of the cerebral cortex. Boston: Birkhauser.

Wierenga CJ, Ibata K, Turrigiano GG (2005) Postsynaptic expression of homeostatic plasticity at neocortical synapses. J Neurosci 25:2895–2905.

Woodhall G, Evans DI, Cunningham MO, Jones RS (2001) NR2B-containing NMDA autoreceptors at synapses on entorhinal cortical neurons. J Neurophysiol 86:1644–1651.

Wu H, Nash JE, Zamorano P, Garner CC (2002) Interaction of SAP97 with minus-end-directed actin motor myosin VI. Implications for AMPA receptor trafficking. J Biol Chem 277:30928–30934.

Wyszynski M, Lin J, Rao A, Nigh E, Beggs AH, Craig AM, Sheng M (1997) Competitive binding of alpha-actinin and calmodulin to the NMDA receptor. Nature 385:439–442.

Zhou Q, Xiao M-Y, Nicoll RA (2001) Contribution of cytoskeleton to the internalization of AMPA receptors. Proc Natl Acad Sci U S A 98:1261–1266.